LAWRENCE
LIVERMORE
NATIONAL
LABORATORY

LLNL-JRNL-796421

Identification of the Molecular-Weight Growth Reaction Network in Counterflow Flames of the C3H4 Isomers Allene and Propyne

G. Kukkadapu, S. W. WaGNON, W. J. Pitz, N. Hansen

November 7, 2019

Proceedings of the combustion Institute

Disclaimer

Identification of the Molecular-Weight Growth Reaction Network in Counterflow Flames of the C_3H_4 Isomers Allene and Propyne

G. Kukkadapu,[1] S. W. Wagnon,[1] W. J. Pitz,[1] N. Hansen[2*]*

[1]Physical and Life Sciences Directorate, Lawrence Livermore National Laboratory, Livermore, CA 94551, USA
[2]Combustion Research Facility, Sandia National Laboratories, Livermore, CA 94551, USA

to be submitted to:

38th International Symposium on Combustion
"Soot Colloquium"

Word Count

Abstract:	183
Introduction:	334
Kinetic modeling:	905
Experimental procedures:	595
Results and discussion:	1825
Conclusion:	188
Acknowledgement:	184
50 References:	909
8 Figures:	1434
Total:	**6200**

Color figures in electronic version only.

Supplementary Material is available.

[*] Corresponding authors: nhansen@sandia.gov, +1 925-294-6272 (NH), kukkadapu1@llnl.gov, +1 925-422-1489 (GK)

LLNL-JRNL-796421

Identification of the Molecular-Weight Growth Reaction Network in Counterflow Flames of the C_3H_4 Isomers Allene and Propyne

G. Kukkadapu,[1] S. W. Wagnon,[1] W. J. Pitz,[1] N. Hansen[2*]*

[1]Physical and Life Sciences Directorate, Lawrence Livermore National Laboratory, Livermore, CA 94551, USA
[2]Combustion Research Facility, Sandia National Laboratories, Livermore, CA 94551, USA

Abstract

The reaction networks responsible for aromatics formation in counterflow flames of the C_3H_4 isomers allene and propyne are identified through a combined experimental and modeling study. Mole fraction profiles of near-atmospheric pressure (933 mbar) diffusion flames fueled by the C_3H_4 isomers are analyzed by means of a newly assembled, chemically detailed kinetic mechanism. The experiment consists of a counterflow burner system that is coupled to a high-resolution time-of-flight molecular-beam mass spectrometer with single-photon ionization via synchrotron-generated vacuum-ultraviolet photons. Flame-sampled, mass-specific photoionization efficiency curves are used to identify the presence of aliphatically substituted aromatic species in addition to the commonly considered pericondensed ring structures. The new mechanism describes the formation and growth of aromatics through repetitive sequences of radical-radical and radical-molecule reactions that include C_1-C_6 intermediates. Higher

concentrations of aromatic species are observed in the allene flame and the new mechanism captures the observed experimental trends very accurately. The results indicate the importance of the aliphatically substituted aromatics and of ring-enlargement reactions for the growth reactions. According to the model simulations, radical+radical recombination and PAH-radical+molecule reactions play an important role in PAH growth.

Keywords: allene; propyne; counterflow flames; PAH formation; chemical modeling

1. Introduction

Formation of soot is still one of the less understood phenomena in combustion. It is agreed upon that the underlying mechanism involves several chemical and physical processes. One of the key chemical processes in the formation of soot is growth of polycyclic aromatic hydrocarbons (PAHs). With the formation of benzene, the simplest aromatic molecule, in combustion processes well understood [1-4], research is now focused on building a more fundamental understanding of the formation of larger aromatic species [5-15].

For many years, the growth of PAHs has been modeled using the celebrated hydrogen-abstraction-C_2H_2-addition (HACA) mechanism. However, recent studies have shown that HACA alone may not be enough to explain the growth of PAHs [7] and additional reaction pathways such as growth by addition reactions with C_3-C_6 species have been suggested [8-15]. The C_3 species have been proposed to facilitate growth by recombination reactions or through formation of C_5 rings [8, 9] which subsequently undergo ring-enlargement reactions to C_6 rings. However, the importance of these reactions in laboratory flames still needs to be verified.

To this end, this study focuses on the chemical structures of two counterflow diffusion flames fueled by the C_3H_4 isomers allene (propadiene, CH_2=C=CH_2) and propyne (methyl-acetylene, CH_3-C≡CH). It is understood that hydrogen-abstraction reactions from these hydrocarbons lead to a resonance-stabilized propargyl radical (C_3H_3), which is a main precursor for formation of first aromatic ring species in combustion processes [1-4, 16]. This study helps explore the role of the propargyl radical (C_3H_3) in growth of larger aromatic species.

Parallel to the experimental analysis of the two flames, a new chemically detailed mechanism has been developed to describe the formation of aromatic ring structures. The

mechanism developed is based on reaction pathways and associated rate parameters from recent high-level *ab-initio* calculations to describe in detail the growth of PAHs using the various repetitive reaction schemes. This detailed PAH mechanism, which is based on fundamental studies, can be useful to gain insights into fuel molecular structure effects on formation and growth of PAHs.

2. Kinetic modeling

Details of the calculations are described in the Supplementary Material. The new PAH mechanism developed (see Supplementary Material) is built on top of LLNL's recent aromatic mechanism [17] with C_0-C_4 chemistry from AramcoMech 2.0 [18]. In the present work, we limit the mechanism to model formation of aromatics up to four aromatic rings. The reaction pathways and the associated reaction rates used to describe the formation of PAHs have been modeled using repetitive reactions schemes taken from recent *ab-initio* studies as described in detail in the following sections.

2.1 Formation of C_6H_6 (benzene and fulvene)

The chemistry describing the formation of benzene and its isomer fulvene is modeled based on the latest literature recommendations and the following reactions are included: 1,3-butadiene+vinyl radical [19], acetylene+C_4H_5 radicals [20], C_3H_3+ C_3H_3 [1], C_3H_3+allyl (C_3H_5-A) radical [2], and cyclopentadienyl (C_5H_5) radical+CH_3 radical [21]. To model the formation of cyclopentadiene and C_5H_5, which are important for the last reaction system, the C_3H_5-A+acetylene [22] and C_3H_3+acetylene [23] reactions have been updated. As the formation of benzene through

the above-mentioned reaction systems is well understood, we shall not provide any further details on these reaction systems here.

2.2 Growth of PAHs beyond benzene

The growth of PAHs has been modeled using repetitive schemes identified in the literature [5-14]. The repetitive reaction schemes for growth of PAH considered are addition of PAH/PAH-radicals with: C_1(methyl radicals); C_2 (acetylene, HACA); C_3 (propene, allene, propyne, propargyl and allyl radicals); C_4 (butadiene and vinylacetylene); C_6 (benzene, phenyl radical, benzyne). This set of reactions is sufficient to explain most intermediate species detected in the flames. To enable a discussion about the reaction networks of PAH formation in the C_3H_4 flames, the following description provides detailed information of molecular growth from reactions of PAHs (and the respective radicals) with C_1-C_6 intermediates as included in the mechanism.

2.2.1 Methyl-assisted growth

The role of methyl radicals in PAH growth can be through a) ipso-substitution reactions with PAHs producing methylated PAHs, b) recombination reactions with PAH radicals producing methyl-substituted PAHs or benzylic radicals, and c) ring-enlargement reactions with resonance-stabilized radicals like cyclopentadienyl and indenyl radicals. The first two reaction classes are known to be important for formation of toluene in both premixed and diffusion flames [3, 24]. The benzylic radicals produced can subsequently react with acetylene leading to formation of indene-like moieties [9] or react with C_3H_3 leading to C_6 rings [25]. The importance of the last reaction sequence c) has been studied earlier by Sharma *et al.* [21] (formation of benzene from C_5H_5), and more recently by Zhao *et al.* [26] (formation of naphthalene from indenyl radical).

2.2.2 HACA-assisted PAH growth

HACA has been widely used to model growth of PAHs and has been studied substantially [27]. In the current mechanism, the HACA scheme has been described using the recent works of Mebel *et al.* [6] and Frenklach *et al.* [28]. The reactions from Ref. [6] have been used to describe addition of acetylene at radical sites on free-edges of PAHs. For addition of acetylene to radical character sites on zig-zag structures, which result in production of cyclopenta-fused PAHs (*e.g.*, 1-naphthyl+C_2H_2⇄acenaphthylene+H), we used the rates from Ref. [29]. For addition of acetylene to PAH radicals with radical character on arm-chair sites (o-biphenyl radical+C_2H_2⇄phenanthrene+H), the rates from Yang *et al.* [13] have been used.

2.2.3 Growth by addition of C_3H_4 isomers and propargyl radicals

The addition of phenyl radicals to C_3H_4 isomers allene and propyne has been revisited recently by Mebel *et al.* [9] who suggested production of a wide distribution of products which include phenylpropynes, phenylallene, phenylacetylene, benzyl radicals, acetylene, methyl radicals, and C_9H_9 adducts. We modeled the phenyl+C_3H_4 reactions according to their findings. As the current diffusion flames contain high amounts of C_3H_3, we also considered the recombination reaction between phenyl and propargyl. The rate for this reaction has been adopted from a recent study of [30].

The reactions of phenyl radical with C_3H_4 isomers and propargyl are expected to produce significant amounts of indene isomers, *i.e.* phenylpropynes and phenylallene, so it is imperative for the mechanism to describe the reactions of these C_9H_8 isomers. Mebel *et al.* [9] explored the addition reactions of C_9H_8 isomers with H radicals but the abstraction of weak allylic hydrogens from these isomers producing resonantly stabilized phenyl-propargyl radicals (PPRs) has not been

studied. We modeled the formation PPRs in our mechanism using analogies from C_3H_4. Furthermore, as PPRs are similar to propargyl radicals we have considered PPR+C_3H_3, PPR+PPR recombination reactions using analogies from the C_3H_3+C_3H_3 system.

2.2.4 Growth by addition of vinylacetylene and 1,3-butadiene

The role of vinylacetylene and 1,3-butadiene towards formation of PAHs has been modeled in the current mechanism using the kinetics from Zhao *et al.* [29] and Fascella *et al.* [10], respectively.

2.2.5 Growth by addition of benzene, phenyl radicals and *o*-benzyne

The reactions of phenyl radicals towards PAH growth has been shown to be important by Shukla [14]. Considering this, we have modeled the PAH+PAH radical reactions using the kinetics from Park *et al.* [31]. Furthermore, the *o*-benzyne assisted growth of PAHs has been modeled using the kinetics provided by Comandini and Brezinsky [32].

2.3 Oxidation of PAHs

The oxidation of PAHs has been modeled according to Singh *et al.* [33] who theoretically studied the oxidation of pyrene radicals. Their study suggested production of embedded resonance-stabilized C_5 rings. The oxidation of these embedded resonance-stabilized C_5 rings has been modeled according to recommendations of Refs. [34, 35].

3. Experimental procedures

The experiments were conducted with Sandia's counterflow burner system which has been explained by Skeen *et al.* [36]. Only limited details are provided here. The burner system comprises two opposing gas outlets which were kept 12 mm apart. Both the allene and propyne non-premixed flames were studied at identical conditions to ensure the temperature and velocity fields were similar. Differences in PAH concentrations can therefore be attributed to the divergent pyrolysis chemistry of allene and propyne. The experiments were conducted at near atmospheric pressure of 700 Torr (933 mbar) in argon dilution with the fuel and oxygen mole fractions of 6.9% and 20% in the fuel and oxidizer stream, respectively. The velocity at the exit of both the nozzles were maintained at 22.12 cm/s.

The flame structures of the C_3H_4 flames were analyzed using high-resolution mass spectrometry with single-photon ionization employing synchrotron-generated vacuum-ultraviolet radiation as described earlier [37, 38]. To this end, the flame gases were sampled via a horizontally mounted quartz nozzle vertically along the centerline of the flame and guided into a two-stage differentially pumped vacuum chamber of the mass spectrometer. The mass spectrometer has a high resolution of ($m/\Delta m \approx 4000$) which allows for separation of the C/H/O elemental composition in the mass range of interest: m/z = 2 u (H_2) to m/z = 204 u ($C_{16}H_{12}$).

Sampling techniques can provide a very accurate and molecule-specific (to some extent even isomer-specific) description of the gas composition in flames. However, these measurements are accompanied with perturbations of the flow- and temperature field around the sampling probe and wall effects, see [39, 40] and references therein. Extensive work has been performed to understand the effect of the sampling probe on low-pressure premixed laminar flames. However,

similar levels of details are missing for atmospheric-pressure diffusion flames. Nevertheless, previous work conveyed impactful insights and quantitative information on PAH-forming combustion chemistry useful for validating combustion chemistry models [37, 38, 41].

Mass-specific photoionization efficiency (PIE) curves were recorded to help with species identification. While this method has been shown to be very successful for small species, given the number of potential isomers for large species, this isomer-resolved approach may not be quantitatively applied for molecules containing more than 7 heavy atoms. There are limitations associated with obtaining isomer-specific information for large molecules, which can be traced back to the exponential growth of conceivable isomers as the number of heavy atoms increases and the expected similarity of photoionization efficiency curves (and ionization energies) [39]. Therefore, an attempt to provide isomer-specific information has not been undertaken. Here, we have used reference PIE curves from Ref. [42] and from Selby and Osborn (private communication) of selected PAHs to qualitatively show the presence of two classes of molecules, *i.e.* the pericondensed ring structures (*e.g.* indene) and the aliphatic PAHs (*e.g.* phenyl-propynes).

To obtain the mole fraction profiles, the data was analyzed as described in Refs. [37-39]. The estimated uncertainty in the reported mole fractions of major intermediates such as methane, ethylene, acetylene, propene, propyne, and benzene is estimated to be below 30%. For larger aromatics, the uncertainty in their mole fractions is estimated to be about a factor of 2. For these aromatics, when photoionization cross sections are typically unavailable, we estimated their cross sections following a common practice in analyzing photoionization mass spectra. Due to missing photoionization cross sections, the uncertainty for larger species could be as high as a factor of 4.

However, the relative uncertainty between the two flames should be considerably smaller given the fact that the same experimental and data reduction procedures were applied.

4. Results and discussion

In this section, we first discuss the PAH species detected in the C_3H_4 flames and their conceivable structures, followed by a discussion on the difference in the propensities of the two isomers to form PAHs. Later, we compare the experimentally determined and simulated mole fractions of the PAHs, and finally discuss reaction pathways important for formation of PAHs in these C_3H_4 flames.

4.1 Flame-sampled mass spectra from allene and propyne flames

The flame-sampled mass spectra for species with a mass-to-charge (*m/z*) ratio greater than 60 from the propyne (top) and the allene (bottom) flames are shown in Fig. 1. As seen, the sample mass spectra measured for the two C_3H_4 flames exhibit striking similarities of the peaks, albeit some differences in the relative intensities of the intermediates. Most of the detected species, *e.g.*, C_6H_6 (*m/z*=78), C_8H_6 (*m/z*=102), $C_{10}H_8$ (*m/z*=128), $C_{12}H_8$ (*m/z*=152), $C_{12}H_{10}$ (*m/z*=154), $C_{14}H_8$ (*m/z*=176), $C_{14}H_{10}$ (*m/z*=178), and $C_{16}H_{10}$ (*m/z*=202), correspond to those on the stabilomer grid identified by Stein and Fahr [43]. However, intermediates were also detected that are not on the stabilomer grid, *e.g.*, C_7H_8 (*m/z*=92), C_9H_8 (*m/z*=116), $C_{10}H_{10}$ (*m/z*=130), $C_{11}H_{10}$ (*m/z*=142), $C_{12}H_{12}$ (*m/z*=156), $C_{13}H_{10}$ (*m/z*=166), $C_{14}H_{12}$ (*m/z*=180), $C_{15}H_{10}$ (*m/z*=190), and $C_{16}H_{12}$ (*m/z*=204). The detection of the non-stabilomer grid molecules agrees with observations by Johansson *et al.* [44].

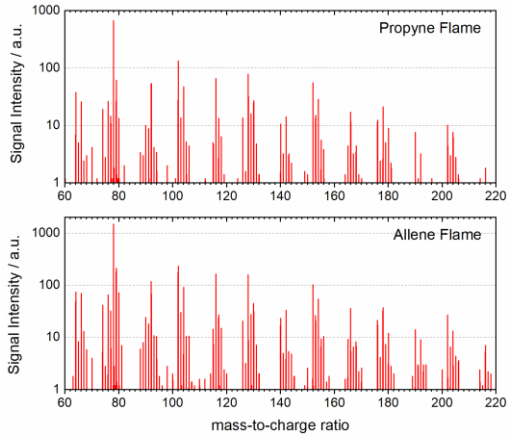

Figure 1: Flame-sampled mass spectra from the propyne (top) and allene (bottom) counterflow diffusion flames. (56x67 mm, 160 words)

Deciphering the underlying chemistry responsible for the molecular weight growth processes requires further insights into the isomeric structures of the C_9H_8 and $C_{13}H_{10}$ detected in the flames. We compared the experimentally recorded PIE curves of C_9H_8 and $C_{13}H_{10}$ isomers with the known PIE curves of different isomers from Zhao *et al.* [42] and Selby and Osborn (personal communication). The flame-sampled photoionization efficiency curves were approximated using a theoretically calculated photoionization efficiency curve $PIE^{calc}(E)$ that is derived using $PIE^{calc}(E) = \sum_i c_i \times PIE^i(E)$, in which i labels the different isomeric species, $PIE^i(E)$ are energy-dependent isomer-specific photoionization efficiency curves, and c_i are the respective weighting factors. $PIE^{calc}(E)$ is referred to as "weighted sum". As seen in Figs. 2a and 2b, the experimentally recorded PIE curves of both C_9H_8 and $C_{13}H_{10}$ could not be replicated by any one isomer alone whilst a weighted sum of the PIE curves of the different isomers provides a best fit. This comparison suggests the potential presence of aliphatic C_9H_8 and $C_{13}H_{10}$ isomers in these flames. Further supporting evidence for this statement is shown in the Supplementary Material where results are shown excluding aliphatic C_9H_8 and $C_{13}H_{10}$ isomers. However, it is to be noted,

that the best fit shown for PIE curves in Fig. 2 is not a unique solution and that the lack of quantitative cross-section data precludes the determination of the isomer specific ratios. While $C_{13}H_{10}$ 1H-benz[f]indene seems to closely match the flame-sampling PIE curve in Fig. 2(b), a single isomeric form is highly unlikely given the complex PAH formation chemistry.

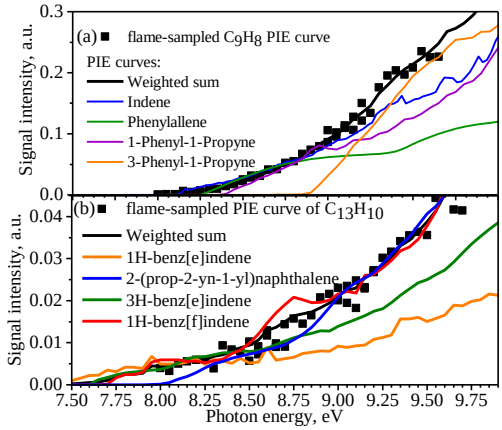

Figure 2: Comparison of PIE curves of (a) C_9H_8 and (b) $C_{13}H_{10}$ from experiments and different molecular isomers. (57x67 mm, 165 words)

The mass spectra intensities have been analyzed and the mole fraction profiles of 20 aromatics (*m/z* between 78 to 204) are provided in the Supplementary Material. For comparison between allene and propyne flames, in Fig. 3 we show the peak mole fractions of species with concentrations more than 10 ppm. Several interesting trends can be seen in Fig. 3: a) mole fractions of non-stabilomer grid molecules such as C_9H_8, $C_{13}H_{10}$ and $C_{15}H_{10}$ are comparable to those on the stabilomer grid, b) the concentrations of $C_{14}H_{10}$ and $C_{16}H_{10}$ are higher than that of the $C_{14}H_8$ stabilomer.

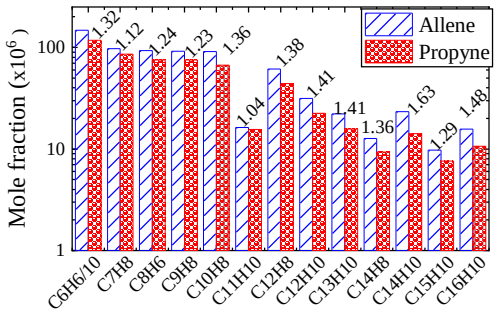

Figure 3: Mole fractions of the different aromatic species detected in the current experiments. The numbers above the bars represent the ratio of peak concentration detected in the two flames (allene/propyne). Mole fraction of C_6H_6 has been divided by 10 in the plot. (41x67 mm, 155 words)

In Fig. 3 we also show the ratio of peak concentrations of PAHs observed in both flames. A ratio greater (smaller) than one would indicate the concentration of PAH is larger (smaller) in the allene flame. As seen in Fig. 3, the ratios are greater than one, suggesting that allene consistently produces higher concentrations of PAHs. This observation corroborates well with the prior premixed flames experiments of Hansen *et al*. [45]. In this earlier work, the authors observed the concentrations of benzene to be higher in an allene flame and the difference was attributed to the relative production of propargyl from allene+H versus propyne+H reactions. The propargyl concentrations, and thereby the benzene concentrations, were found to be higher in the allene flame while acetylene and methyl/methane (derived from propyne+H$\rightleftarrows C_2H_2+CH_3$) were higher in the propyne flame. The comparison of the acetylene, methane, and benzene mole fractions from experiments and modeling results in this work show similar trends as shown next.

4.2. Overall mechanism performance

The comparison of the experimental and simulated mole fractions of selected species is shown in Fig. 4. Additional species profiles are shown in the Supplementary Material. As seen, the performance of the PAH mechanism relative to the measurements is very encouraging with differences in mole fractions of most species within a factor of 2. It should be noted that this factor of 2 difference in mole fraction is about the measurement uncertainty for PAHs with known photoionization cross sections (up to a factor 4 for species with unknown cross sections). This level of agreement between experimental results and model predictions in peak mole fraction and position is expected. A better (or even a perfect) agreement cannot be expected given our current understanding of the molecular-weight growth chemistry, experimental limitations, and the simulation approach. The reported discrepancies indicate potential gaps in our current chemical knowledge of molecular-weight growth processes.

However, the differences in mole fractions of methane and toluene appear to be outside the experimental uncertainties. Nevertheless, the trends are reproduced correctly. That is, although the mechanism underpredicts the concentrations of toluene (C_7H_8), the sensitivity of the toluene formation to fuel structure is accurately predicted. To elaborate, the experiments suggest the concentrations of toluene to be less sensitive to the fuel structure (a ratio of the peak concentrations of 1.12 was observed), and this trend is well predicted by the mechanism. The difference in concentrations of methane is surprising and could result from possible shortcomings in the methane chemistry of AramcoMech 2.0 [18].

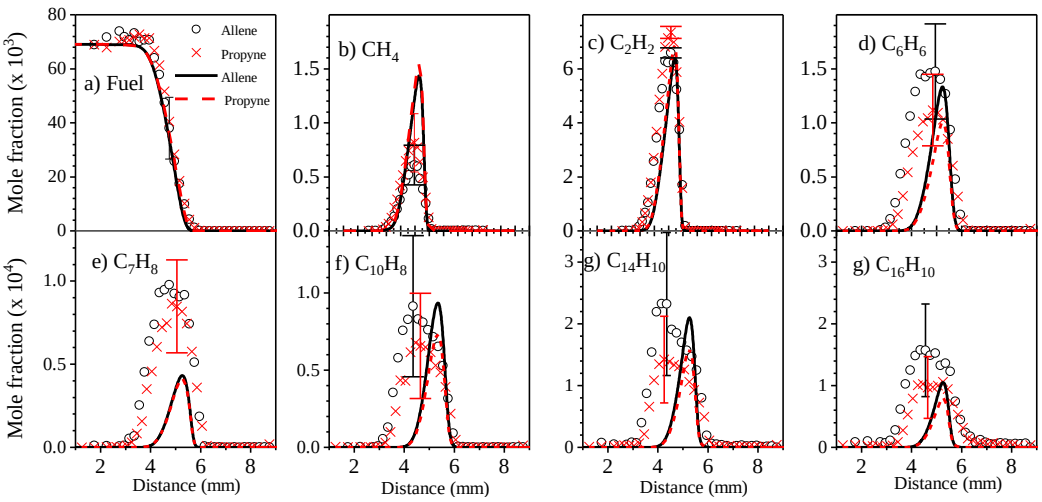

Figure 4: Comparison of mole fractions of the fuel, C_2H_2, CH_4, benzene isomers (C_6H_6), phenylacetylene (C_8H_6), toluene (C_7H_8), and selected PAHs from experiments (symbols) and simulations (lines). (66x144 mm, 361 words)

For comparisons shown in Fig. 4, a shift in peak location and earlier buildup of PAHs is noticed when compared against simulations. These discrepancies in the profile shapes could be caused by several effects which include shortcomings in the mechanism, sampling probe perturbations, and non-idealities in flow field at nozzle exit [46]. Such experimental non-idealities are not reflected in the current numerical model.

4.3 Molecular-weight growth reaction network

We conducted integrated rate of production analysis to identify the reaction pathways important for PAH growth. A main finding was the importance of aliphatic- and non-stabilomer grid molecules towards formation of biphenyl, naphthalene, and phenanthrene through ring-enlargement and radical-radical recombination reactions as hypothesized in Ref. [47]. We shall discuss this important network herein. In addition to radical-radical recombination reactions, we also found PAH molecule+PAH radical reactions to be important and they shall be discussed. We

begin with the identification of pathways important for formation of C_9H_8 and $C_{13}H_{10}$ isomers (produced through growth reactions on phenyl and naphthyl radicals), and show their importance towards formation of biphenyl, naphthalene, and phenanthrene. In the following discussions, we focus only on the propyne flame as both flames exhibit a similar PAH growth network.

4.3.1 Isomeric distribution of C_9H_8 and $C_{13}H_{10}$ and their role in PAH growth

Comparisons of the simulated mole fractions of the different isomers of C_9H_8 and $C_{13}H_{10}$ and the total simulated and experimental mole fractions of C_9H_8 and $C_{13}H_{10}$ are shown in Fig. 5. Based on the model predictions, ~80% of the C_9H_8 and $C_{13}H_{10}$ in the flames are indene and benzo-indenes (9-fluorene/1H-benz[e]indene/3H-benz[e]indene/1H-benz[f]indene) respectively, and the remaining 20% are propynyl-/allenyl- substituted benzene and naphthalene respectively. As the simulated peaks for the $C_{13}H_{10}$ isomers show a larger discrepancy when compared against C_9H_8 isomers, the conclusion on the relative importance of the aliphatic $C_{13}H_{10}$ isomers might seem uncertain. However, based on our current understanding that PAH growth chemistry is driven by repetitive schemes [5], comparison of PIE curves (c.f., Fig. 2) and the known similarity in the reactions of phenyl and naphthyl radicals [4] with C_3 species, we can confidently state that aliphatic $C_{13}H_{10}$ isomers are present.

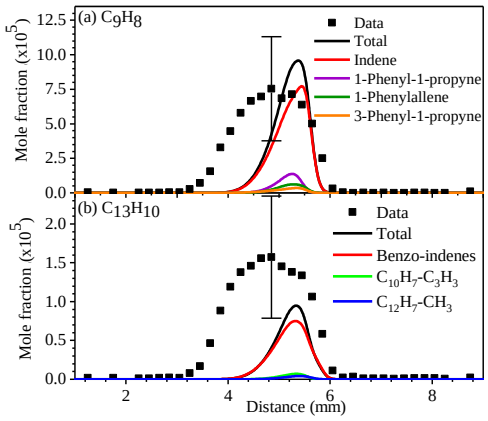

Figure 5: Comparison of simulated mole fractions of different (a) C_9H_8 and (b) $C_{13}H_{10}$ isomers in the propyne flame. (57x67 mm, 166 words)

From the comparison of mole-fractions it might appear that formation of aliphatic C_9H_8, $C_{13}H_{10}$ may not be important. However, in the flux analysis we observed that indene and benzo-indenes (and their radicals) are dominantly produced from cyclization of aliphatic C_9H_8 and $C_{13}H_{10}$. For C_9H_8 isomers we show this reaction sequence in Fig. 6, which illustrates the importance of recombination reaction between aryl and propargyl radicals.

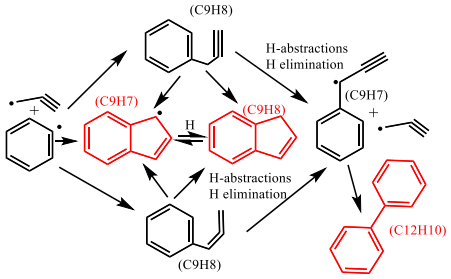

Figure 6: Role of aliphatic C_9H_8 isomers towards formation of indene and biphenyl. (43x67 mm, 130 words)

As discussed in section 2.2.3, the H-abstractions from the aliphatic side chain produce phenyl-propargyl (PPR, C_6H_5CHCCH) radicals. From the current model we find the PPR+C_3H_3 recombination reaction, as proposed earlier by Stein *et al.* [48], to be important for predicting the concentrations of $C_{12}H_{10}$ isomers (see Fig. 7). PPR can also be produced from phenyl+C_3H_3 reaction via the pathways shown in Fig. 6. The comparison shown in Fig. 7 highlights the potential importance of PPR on growth of PAHs and the need for better understanding of their chemistry.

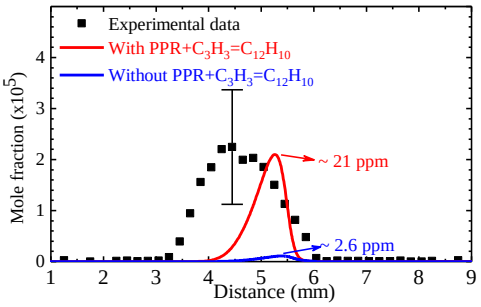

Figure 7: Effect of PPR+C_3H_3 reaction on concentration of $C_{12}H_{10}$ isomers. (41x67 mm, 124 words)

4.4 Role of ring-enlargement reactions in formation of naphthalene and phenanthrene

To gain further insights into PAH growth, we show the summary of the flux analysis for formation of naphthalene and phenanthrene in Figs. 8a and 8b. As seen, the indenyl+CH_3, and benzoindenyl+CH_3 reactions via ring-enlargement schemes contribute significantly to formation of naphthalene and phenanthrene, respectively. Detection of $C_{12}H_{12}$, $C_{13}H_{10}$, $C_{14}H_{12}$, $C_{15}H_{10}$, and $C_{16}H_{12}$ in the mass spectra shown in Fig. 1 provide evidence for these ring-enlargement reactions. Figure 8a also shows the importance of fulvenallenyl radical (C_7H_5) towards growth of naphthalene. The C_7H_5+C_3H_3 was proposed by da Silva and Bozzelli [49] to be important for

pyrolysis of toluene, and according to them is similar to the recombination reaction of propargyl radicals. However, detailed and the reaction rates of $C_7H_5+C_3H_3$ reaction have not been reported. Given its importance it would be recommended to theoretically study this reaction.

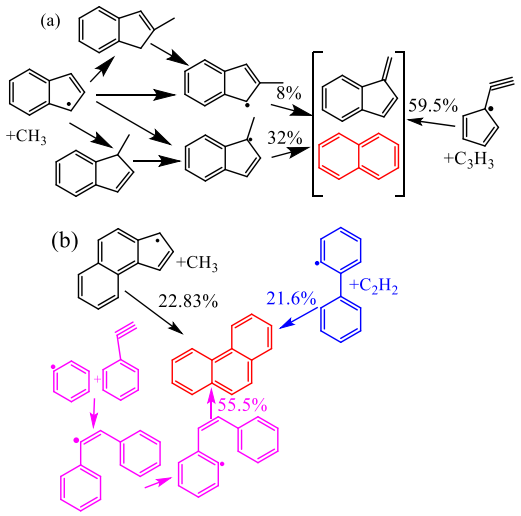

Figure 8: Fluxes of important pathways for formation of (a) naphthalene and (b) phenanthrene. (63x67 mm, 173 words)

In addition to the ring-enlargement reaction, biphenyl and phenylacetylene also contribute towards formation of phenanthrene (also shown in Fig. 8b). The addition of phenyl radical to phenylacetylene in the current mechanism has been modeled according to recommendations of Ref. [11]. However, Parker *et al.* [50] did not notice phenanthrene to be a major product in their cross-beam experiments, and the importance of this reaction towards formation of phenanthrene is still not clear. Considering that this addition reaction supports fast PAH growth, it might be worth revisiting this reaction.

Finally, the analysis of the experimental data and simulations conducted here highlight the role of propargyl radical and ring-enlargement reactions in formation of non-stabilomer grid molecules and PAH with C_6 rings. To further test the importance of these pathways, simulations were conducted with the current mechanism considering HACA only, ignoring the role of

propargyl radicals and ring enlargement mechanisms. In these simulations, the concentrations of the PAHs were found to be severely underpredicted (shown in the Supplementary Material). This analysis shows the need to incorporate the reactions of propargyl radical with aryl radicals and ring-enlargement reaction pathways in kinetic mechanisms used to model formation of PAH growth.

5. Conclusions

A combined experimental and modeling study was performed to understand the reaction growth network of PAH formation in counterflow diffusion flames of allene and propyne. To this end, a new chemically detailed mechanism was constructed which describes the formation and growth reactions through repetitive sequences of radical-radical and radical-molecule reactions that include C_1-C_6 intermediates. The experimental measurements show the effect of isomeric structures on formation of PAHs, and the detection of stabilomer grid and odd carbon containing non-stabilomer grid molecules in flames. The concentrations of the non-stabilomer grid molecules were found to be comparable to that of stabilomer grid molecules. Comparison of photoionization efficiency curves suggest the presence of aliphatic substituted PAHs. The detailed chemical mechanism reproduces the observed experimental trends and the concentrations of the PAHs satisfactorily. The reaction path analysis conducted with the detailed mechanism reveals the importance of radical+radical recombination, PAH-radical+molecule and of the aliphatic substituted aromatics towards formation of aliphatic-substituted PAHs, non-stabilomer and stabilomer grid molecules. The inclusion of these repetitive reaction growth networks in kinetic

models may significantly aid efforts to simulate PAH, and ultimately soot, formation in practical combustion applications.

Acknowledgements

NH acknowledges support from the U.S. DOE, Office of Science, Office of Basic Energy Sciences. Sandia National Laboratories is a multi-mission laboratory managed and operated by National Technology and Engineering Solutions of Sandia, LLC., a wholly owned subsidiary of Honeywell International, Inc., for the U.S. Department of Energy's National Nuclear Security Administration under contract DE-NA0003525. The authors gratefully acknowledge Paul Fugazzi for technical assistance. The experiments were conducted at the Advance Light Berkeley, Berkeley National Laboratory, Berkeley, CA, USA. The Advanced Light Source is supported by the Director, Office of Science, Office of Basic Energy Sciences, of the U.S. DOE under Contract No. DEAC02-05CH11231. The work at LLNL was performed under the auspices of the U.S. Department of Energy (DOE), Contract DE-AC52-07NA27344 and was supported by the U.S. Department of Energy, Office of Basic Energy Sciences and Vehicle Technologies Office, program managers Wade Sisk, Kevin Stork, Mike Weismiller and Gurpreet Singh and was conducted as part of the Co-Optimization of Fuels & Engines (Co-Optima) project sponsored by the DOE Office of Energy Efficiency and Renewable Energy (EERE), Bioenergy Technologies and Vehicle Technologies Offices.

References

[1] J.A. Miller; S.J. Klippenstein, *The recombination of propargyl radicals and other reactions on a C_6H_6 potential.* Journal of Physical Chemistry A 107 (39) (2003) 7783-7799.

[2] J.A. Miller; S.J. Klippenstein; Y. Georgievskii; L.B. Harding; W.D. Allen; A.C. Simmonett, *Reactions between resonance-stabilized radicals: Propargyl plus allyl.* Journal of Physical Chemistry A 114 (14) (2010) 4881-4890.

[3] N. Hansen; J.A. Miller; S.J. Klippenstein; P.R. Westmoreland; K. Kohse-Höinghaus, *Exploring formation pathways of aromatic compounds in laboratory-based model flames of aliphatic fuels.* Combustion Explosion and Shock Waves 48 (5) (2012) 508-515.

[4] C.S. McEnally; L.D. Pfefferle; B. Atakan; K. Kohse-Höinghaus, *Studies of aromatic hydrocarbon formation mechanisms in flames: Progress towards closing the fuel gap.* Progress in Energy and Combustion Science 32 (3) (2006) 247-294.

[5] N. Hansen; M. Schenk; K. Moshammer; K. Kohse-Höinghaus, *Investigating repetitive reaction pathways for the formation of polycyclic aromatic hydrocarbons in combustion processes.* Combustion and Flame 180 (2017) 250-261.

[6] A.M. Mebel; Y. Georgievskii; A.W. Jasper; S.J. Klippenstein, *Temperature-and pressure-dependent rate coefficients for the HACA pathways from benzene to naphthalene.* Proceedings of the Combustion Institute 36 (1) (2017) 919-926.

[7] V. Kislov; A. Sadovnikov; A. Mebel, *Formation mechanism of polycyclic aromatic hydrocarbons beyond the second aromatic ring.* Journal of Physical Chemistry A 117 (23) (2013) 4794-4816.

[8] V. Kislov; A. Mebel; J. Aguilera-Iparraguirre; W.H. Green, *Reaction of phenyl radical with propylene as a possible source of indene and other polycyclic aromatic hydrocarbons: An ab initio/RRKM-ME study.* Journal of Physical Chemistry A 116 (16) (2012) 4176-4191.

[9] A.M. Mebel; Y. Georgievskii; A.W. Jasper; S.J. Klippenstein, *Pressure-dependent rate constants for PAH growth: formation of indene and its conversion to naphthalene.* Faraday Discussions 195 (2017) 637-670.

[10] S. Fascella; C. Cavallotti; R. Rota; S. Carrà, *Quantum chemistry investigation of key reactions involved in the formation of naphthalene and indene.* Journal of Physical Chemistry A 108 (17) (2004) 3829-3843.

[11] J. Aguilera-Iparraguirre; W. Klopper, *Density functional theory study of the formation of naphthalene and phenanthrene from reactions of phenyl with vinyl-and phenylacetylene.* Journal of chemical theory and computation 3 (1) (2007) 139-145.

[12] R.S. Tranter; S.J. Klippenstein; L.B. Harding; B.R. Giri; X. Yang; J.H. Kiefer, *Experimental and theoretical investigation of the self-reaction of phenyl radicals.* Journal of Physical Chemistry A 114 (32) (2010) 8240-8261.

[13] T. Yang; R.I. Kaiser; T.P. Troy; B. Xu; O. Kostko; M. Ahmed; A.M. Mebel; M.V. Zagidullin; V.N. Azyazov, *HACA's heritage: A free-radical pathway to phenanthrene in circumstellar envelopes of asymptotic giant branch stars.* Angewandte Chemie-International Edition 129 (16) (2017) 4586-4590.

[14] B. Shukla; A. Susa; A. Miyoshi; M. Koshi, *Role of phenyl radicals in the growth of polycyclic aromatic hydrocarbons.* Journal of Physical Chemistry A 112 (11) (2008) 2362-2369.

[15] C. Cavallotti; D. Polino; A. Frassoldati; E. Ranzi, *Analysis of some reaction pathways active during cyclopentadiene pyrolysis.* Journal of Physical Chemistry A 116 (13) (2012) 3313-3324.

[16] Y. Georgievskii; J.A. Miller; S.J. Klippenstein, *Association rate constants for reactions between resonance-stabilized radicals: $C_3H_3+C_3H_3$, $C_3H_3+C_3H_5$, and $C_3H_5+C_3H_5$.* Physical Chemistry Chemical Physics 9 (31) (2007) 4259-4268.

[17] G. Kukkadapu; D. Kang; S.W. Wagnon; K. Zhang; M. Mehl; M. Monge-Palacios; H. Wang; S.S. Goldsborough; C.K. Westbrook; W.J. Pitz, *Kinetic modeling study of surrogate components for gasoline, jet and diesel fuels: C_7-C_{11} methylated aromatics.* Proceedings of the Combustion Institute 37 (1) (2019) 521-529.

[18] Y. Li; C.-W. Zhou; K.P. Somers; K. Zhang; H.J. Curran, *The oxidation of 2-butene: A high pressure ignition delay, kinetic modeling study and reactivity comparison with isobutene and 1-butene.* Proceedings of the Combustion Institute 36 (1) (2017) 403-411.

[19] Z.J. Buras; E.E. Dames; S.S. Merchant; G. Liu; R.M. Elsamra; W.H. Green, *Kinetics and products of vinyl+1,3-butadiene, a potential route to benzene.* Journal of Physical Chemistry A 119 (28) (2015) 7325-7338.

[20] J.P. Senosiain; J.A. Miller, *The Reaction of n-and i-C_4H_5 Radicals with Acetylene.* Journal of Physical Chemistry A 111 (19) (2007) 3740-3747.

[21] S. Sharma; W.H. Green, *Computed rate coefficients and product yields for c-C_5H_5+CH_3→ products.* Journal of Physical Chemistry A 113 (31) (2009) 8871-8882.

[22] K. Wang; S.M. Villano; A.M. Dean, *Experimental and kinetic modeling study of butene isomer pyrolysis: Part I. 1-and 2-Butene.* Combustion and Flame 173 (2016) 347-369.

[23] G. da Silva, *Mystery of 1-vinylpropargyl formation from acetylene addition to the propargyl radical: an open-and-shut case.* Journal of Physical Chemistry A 121 (10) (2017) 2086-2095.

[24] N. Hansen; X. He; R. Griggs; K. Moshammer, *Knowledge generation through data research: New validation targets for the refinement of kinetic mechanisms.* Proceedings of the Combustion Institute 37 (1) (2019) 743-750.

[25] A. Matsugi; A. Miyoshi, *Computational study on the recombination reaction between benzyl and propargyl radicals.* International Journal of Chemical Kinetics 44 (3) (2012) 206-218.

[26] L. Zhao; R.I. Kaiser; W. Lu; B. Xu; M. Ahmed; A.N. Morozov; A.M. Mebel; A.H. Howlader; S.F. Wnuk, *Molecular mass growth through ring expansion in polycyclic aromatic hydrocarbons via radical–radical reactions.* Nature Communications 10 (1) (2019) 1-7.

[27] H. Wang, *Formation of nascent soot and other condensed-phase materials in flames.* Proceedings of the Combustion Institute 33 (1) (2011) 41-67.

[28] M. Frenklach; R.I. Singh; A.M. Mebel, *On the low-temperature limit of HACA.* Proceedings of the Combustion Institute 37 (1) (2019) 969-976.

[29] L. Zhao; R.I. Kaiser; B. Xu; U. Ablikim; M. Ahmed; M.V. Zagidullin; V.N. Azyazov; A.H. Howlader; S.F. Wnuk; A.M. Mebel, *VUV photoionization study of the formation of the simplest polycyclic aromatic hydrocarbon: Naphthalene ($C_{10}H_8$).* Journal of Physical Chemistry Letters 9 (10) (2018) 2620-2626.

[30] A.N. Morozov; A.M. Mebel, *Theoretical study of the reaction mechanism and kinetics of the phenyl+ propargyl association.* Physical Chemistry Chemical Physics 22 (13) (2020) 6868-6880.

[31] J. Park; S. Burova; A. Rodgers; M. Lin, *Experimental and theoretical studies of the C_6H_5+C_6H_6 reaction.* Journal of Physical Chemistry A 103 (45) (1999) 9036-9041.

[32] A. Comandini; K. Brezinsky, *Theoretical study of the formation of naphthalene from the radical/π-bond addition between single-ring aromatic hydrocarbons.* Journal of Physical Chemistry A 115 (22) (2011) 5547-5559.

[33] R.I. Singh; A.M. Mebel; M. Frenklach, *Oxidation of graphene-edge six-and five-member rings by molecular oxygen.* Journal of Physical Chemistry A 119 (28) (2015) 7528-7547.

[34] G. Galimova; V. Azyazov; A. Mebel, *Reaction mechanism, rate constants, and product yields for the oxidation of cyclopentadienyl and embedded five-member ring radicals with hydroxyl.* Combustion and Flame 187 (2018) 147-164.

[35] A. Ghildina; A. Oleinikov; V. Azyazov; A. Mebel, *Reaction mechanism, rate constants, and product yields for unimolecular and H-assisted decomposition of 2, 4-cyclopentadienone and oxidation of cyclopentadienyl with atomic oxygen.* Combustion and Flame 183 (2017) 181-193.

[36] S.A. Skeen; H.A. Michelsen; K.R. Wilson; D.M. Popolan; A. Violi; N. Hansen, *Near-threshold photoionization mass spectra of combustion-generated high-molecular-weight soot precursors.* Journal of Aerosol Science 58 (2013) 86-102.

[37] K. Moshammer; L. Seidel; Y. Wang; H. Selim; S.M. Sarathy; F. Mauss; N. Hansen, *Aromatic ring formation in opposed-flow diffusive 1,3-butadiene flames.* Proceedings of the Combustion Institute 36 (1) (2017) 947-955.

[38] L. Ruwe; K. Moshammer; N. Hansen; K. Kohse-Höinghaus, *Influences of the molecular fuel structure on combustion reactions towards soot precursors in selected alkane and alkene flames.* Physical Chemistry Chemical Physics 20 (16) (2018) 10780-10795.

[39] F.N. Egolfopoulos; N. Hansen; Y. Ju; K. Kohse-Höinghaus; C.K. Law; F. Qi, *Advances and challenges in laminar flame experiments and implications for combustion chemistry.* Progress in Energy and Combustion Science 43 (2014) 36-67.

[40] N. Hansen; R.S. Tranter; K. Moshammer; J.B. Randazzo; J.P.A. Lockhart; P.G. Fugazzi; T. Tao; A. Kastengren, *2D-Imaging of Sampling-Probe Perturbations in Laminar Premixed Flames using Kr X-ray Fluorescence.* Combust. Flame 181 (2017) 214-224.

[41] B.D. Adamson; S.A. Skeen; M. Ahmed; N. Hansen, *Detection of aliphatically bridged multi-core polycyclic aromatic aydrocarbons in sooting flames with atmospheric-sampling high-resolution tandem mass spectrometry*. Journal of Physical Chemistry A 122 (48) (2018) 9338-9349.

[42] L. Zhao; M. Prendergast; R.I. Kaiser; B. Xu; U. Ablikim; W. Lu; M. Ahmed; A.D. Oleinikov; V.N. Azyazov; A.H. Howlader, *How to add a five-membered ring to polycyclic aromatic hydrocarbons (PAHs)–molecular mass growth of the 2-naphthyl radical ($C_{10}H_7$) to benzindenes ($C_{13}H_{10}$) as a case study.* Physical Chemistry Chemical Physics 21 (30) (2019) 16737-16750.

[43] S.E. Stein; A. Fahr, *High-temperature stabilities of hydrocarbons.* Journal of Physical Chemistry A 89 (17) (1985) 3714-3725.

[44] K.O. Johansson; J.Y.W. Lai; S.A. Skeen; D.M. Popolan-Vaida; K.R. Wilson; N. Hansen; A. Violi; H.A. Michelsen, *Soot precursor formation and limitations of the stabilomer grid.* Proceedings of the Combustion Institute 35 (2015) 1819-1826.

[45] N. Hansen; J.A. Miller; C.A. Taatjes; J. Wang; T.A. Cool; M.E. Law; P.R. Westmoreland, *Photoionization mass spectrometric studies and modeling of fuel-rich allene and propyne flames.* Proceedings of the Combustion Institute 31 (2007) 1157-1164.

[46] C. Sung; J. Kistler; M. Nishioka; C.K. Law, *Further studies on effects of thermophoresis on seeding particles in LDV measurements of strained flames.* Combustion and Flame 105 (1-2) (1996) 189-201.

[47] K. Johansson; M. Head-Gordon; P. Schrader; K. Wilson; H. Michelsen, *Resonance-stabilized hydrocarbon-radical chain reactions may explain soot inception and growth.* Science 361 (6406) (2018) 997-1000.

[48] S.E. Stein; J.A. Walker; M.M. Suryan; A. Fahr, *A new path to benzene in flames.* Proceedings of the Combustion Institute 23 (1) (1991) 85-90.

[49] G. da Silva; J.W. Bozzelli, *The C7H5 fulvenallenyl radical as a combustion intermediate: Potential new pathways to two-and three-ring pahs.* Journal of Physical Chemistry A 113 (44) (2009) 12045-12048.

[50] D.S. Parker; T. Yang; R.I. Kaiser; A. Landera; A.M. Mebel, *On the formation of ethynylbiphenyl ($C_{14}D_5H_5$; $C_6D_5C_6H_4CCH$) isomers in the reaction of D_5-phenyl radicals (C_6D_5; X^2A_1) with phenylacetylene ($C_6H_5C_2H$; X^1A_1) under single collision conditions.* Chemical Physics Letters 595 (2014) 230-236.